



Open Archive TOULOUSE Archive Ouverte (OATAO)

OATAO is an open access repository that collects the work of Toulouse researchers and makes it freely available over the web where possible.

This is an author-deposited version published in : <http://oatao.univ-toulouse.fr/>
Eprints ID : 11513

To link to this article : doi:10.1029/2012JG001992
URL : <http://dx.doi.org/10.1029/2012JG001992>

To cite this version : Rydberg, Johan and Rosén, Peter and Lambertsson, Lars and De Vleeschouwer, François and Tomasdotter, Sophia and Bindler, Richard Assessment of the spatial distributions of total- and methyl-mercury and their relationship to sediment geochemistry from a whole-lake perspective. (2012) Journal of Geophysical Research, vol. 117 (n° G4). ISSN 0148-0227

Any correspondance concerning this service should be sent to the repository administrator: staff-oatao@listes-diff.inp-toulouse.fr

Assessment of the spatial distributions of total- and methyl-mercury and their relationship to sediment geochemistry from a whole-lake perspective

J. Rydberg,¹ P. Rosén,² L. Lambertsson,³ F. De Vleeschouwer,^{1,4} S. Tomasdotter,¹ and R. Bindler¹

[1] The aim of this study was to determine the spatial variability for total- and methylmercury in surface sediments (0–2 cm) across a single whole-lake basin, and to relate this variability to the sediment's geochemical composition. 83 surface sediment samples from Stor-Strömsjön – a lake with multiple sub-basins located in northern Sweden – were analyzed for geochemical composition as well as total-mercury (total-Hg) and methylmercury (methyl-Hg; 35 samples) concentrations. Our results indicate that variations in fine-grained mineral matter (36%) and organic matter (34%) explain an equal amount of the total-Hg variation, but that their relative importance varies between different parts of the lake. Total-Hg concentrations were similar in locations controlled by organic matter or fine-grained mineral matter (average 109 ng g⁻¹); however, total-Hg inventories (mass per unit area) were significantly higher in the latter (35 and 53 μg m⁻², respectively). Methyl-Hg concentrations are largely (55% of variance) controlled by water depth and sulfur concentration, which supports the importance of within lake methylation reported from other studies. Both for concentrations and inventories the spatial distribution for methyl-Hg in surface sediments is patchy, and interestingly the highest methyl-Hg inventory (1.4 μg m⁻²) was found in a shallow location with coarse-grained minerogenic sediment (very low organic matter). A large spatial variability, even within a single lake, is something that needs to be recognized, e.g., when studying processes affecting mercury cycling, mercury loadings and when using lake sediments to reconstruct historic mercury deposition.

Citation: Rydberg, J., P. Rosén, L. Lambertsson, F. De Vleeschouwer, S. Tomasdotter, and R. Bindler (2012), Assessment of the spatial distributions of total- and methyl-mercury and their relationship to sediment geochemistry from a whole-lake perspective,

1. Introduction

[2] Mercury (Hg) and its cycling has been studied from a wide range of different perspectives, and the research community currently possesses a broad knowledge on the behavior of Hg in the environment. In brief: Hg is largely added to the environment through atmospheric deposition upon the terrestrial landscape [Hines and Brezonik, 2007; Lindqvist et al., 1991]. Because Hg has a high affinity for organic matter, Hg storage in soils and transport to streams

and lakes are largely coupled with that of organic matter [Gabriel and Williamson, 2004; Skyllberg et al., 2006]. Upon entering lakes a large part of the Hg is accumulated in sediments [Hines and Brezonik, 2007]; these sediments can be used as archives to reconstruct Hg deposition history [Bindler et al., 2001a; Fitzgerald et al., 1998; Phillips et al., 2011; Swain et al., 1992] and to calculate Hg budgets for the lake and its catchment [Fitzgerald et al., 2005; Yang et al., 2002]. Under anoxic conditions, for example, in mires, hypolimnetic waters and sediments, Hg can be methylated [Branfireun et al., 1999; Eckley and Hintelmann, 2006; Gilmour et al., 1992]. The methylated Hg can then readily enter the food-web and be enriched in higher trophic levels [Benoit et al., 2003; Ullrich et al., 2001]. However, even with this extensive knowledge it has proven difficult to fully account for variations in Hg and methyl-Hg (MeHg) within and between lakes, both in sediments and in fish [Rypel et al., 2008; Wiener et al., 2006].

[3] One aspect that is rarely fully considered is spatial variability in total-Hg and methyl-Hg accumulation within single lakes. Except for lakes with very small catchment to

¹Department of Ecology and Environmental Science, Umeå University, Umeå, Sweden.

²Climate Impacts Research Centre, Department of Ecology and Environmental Science, Umeå University, Abisko, Sweden.

³Department of Chemistry, Umeå University, Umeå, Sweden.

⁴EcoLab, UMR 5245, CNRS-UPS-INPT, Castanet-Tolosan, France.

Corresponding author: J. Rydberg, Department of Ecology and Environmental Science, Umeå University, SE-90187 Umeå, Sweden. (johan.rydberg@emg.umu.se)

lake area ratios, Hg is largely added to the environment through deposition of inorganic Hg on the terrestrial part of a lake's catchment, and over time some of this Hg is transported from the catchment to the lake [Hines and Brezonik, 2007; Lindqvist et al., 1991]. In the boreal landscape this transport is generally assumed to be tightly coupled with the transport of organic matter [Benoit et al., 2003; Gabriel and Williamson, 2004; Skjellberg et al., 2006]. Upon entering the lake a governing assumption for the within-lake distribution of organic matter, and hence also Hg, is that it is controlled by sediment focusing [Likens and Davis, 1975]. This generalized model for sedimentation describes a preferential transport of light, fine-grained material such as organic matter from shallower to deeper areas of a lake [Håkanson and Jansson, 1983; Likens and Davis, 1975], and the main drivers are considered to be basin slope, water depth and wave action [Blais and Kalff, 1995; Rowan et al., 1992]. However, not all lakes seem to fully comply with this generalized model. In part this can be explained by catchment characteristics having a significant effect on the quality and amount of the organic matter accumulated at nearshore locations [Korsman et al., 1999]. It has also been shown that shallow-water vegetation [Benoy and Kalff, 1999], complex basin morphometry (e.g., multiple basins and islands) and prevailing wind directions [Bindler et al., 2001b] can have a strong influence on the spatial distribution of organic matter as well as Hg and lead (Pb).

[4] Because methylation is primarily a microbially mediated process, the formation of methyl-Hg in the sediment is determined by, for example, available Hg, number of viable methylating bacteria cells, presence of suitable substrate and the chemical conditions [Benoit et al., 2003; Ullrich et al., 2001]. Hence, if the sediment - both its organic and inorganic fractions - is spatially variable then methylation, and thus, methyl-Hg concentrations will also likely vary greatly across the lake bottom. This spatially variable in situ net production of methyl-Hg will then be superimposed on the spatially variable inputs of methyl-Hg to the sediment from other sources (e.g., terrestrial or water column [Branfireun et al., 2005; Eckley and Hintelmann, 2006]). Taken together this suggests that the spatial distribution for methyl-Hg can be very complex in lakes, which might have important implications for Hg bioavailability in different parts of the lake [Chételat et al., 2011].

[5] The spatial distribution of Hg in whole-lake basins has previously been studied both from the perspective of understanding total-Hg mass balance at a catchment or regional scale [Fitzgerald et al., 2005; Swain et al., 1992; Yang et al., 2002] and to investigate the relation between total- and methyl-Hg and other sediment variables, for example, organic matter, grain size, lake-basin morphometry, pH and redox conditions [Croston et al., 1996; Ethier et al., 2010; Feyte et al., 2011; Kainz and Lucotte, 2006; Rhoton and Bennett, 2009]. However, for most studies a relatively low number of sampling sites were used ($n = 1-17$), and most often these sites were distributed along a single transect from shallow to deep waters. The combination of a low sample number and the exclusion of, for example, shallow embayments introduce a risk of not capturing the true range of spatial variability in the studied lakes [cf. Bindler et al., 2001b; Korsman et al., 1999; Rippey et al., 2008]. In the rare occasion where a large number of samples (50) have

been used [Rada et al., 1993], the selected study sites were small lakes with simple basin morphometry, something that might oversimplify the observed patterns. In most studies there is also a tendency to focus on the organic fraction of the sediment, and thus, neglecting the inorganic fraction, which can be of large importance in determining, for example, the Hg bioavailability [Gabriel and Williamson, 2004].

[6] In the present study we aimed to take one step back and revisit fundamental questions of how the solid phase sediment composition - and especially total-Hg and methyl-Hg - varies spatially across a complex lake basin. Our specific research questions were: (i) How variable is the sediment composition within a single lake? (ii) What are the distribution patterns for total-Hg and methyl-Hg across the lake basin? (iii) Can the distribution of total-Hg and methyl-Hg be linked to the physical (i.e., bulk density and water depth) and geochemical properties (concentrations for 28 major and trace elements) of the sediment material, and if so, what are the most important links?

[7] In order to achieve our objective we collected surface sediment samples across the whole basin of the lake Stor-Strömsjön, a small boreal lake with two basins located in northern Sweden. We measured total- and methyl-Hg and characterized the geochemical composition of the sediment matrix using elemental analysis, wavelength dispersive X-ray fluorescence spectrometry (WD-XRF) and Fourier-transform infrared spectrometry (FTIRS). Finally the Hg data were coupled with the geochemical data and subjected to exploratory multivariate statistics (cluster analysis and principal component analysis (PCA)). These statistical tools help us to see beyond individual elements and thereby treat the sediment matrix as a complex unit that can be related, statistically, to the total-Hg and methyl-Hg distributions.

2. Materials and Methods

2.1. Study Site

[8] Stor-Strömsjön (64°07'N, 19°14'E, 209 m.a.s.l) is a relatively small, dimictic lake situated in northern Sweden, approximately 60 km NW of Umeå. Mean annual air temperature for the area is $\sim 3^{\circ}\text{C}$ (SMHI). The area consists of old, slow-weathering metamorphic bedrock covered with poorly sorted glacial till (www.sgu.se). The catchment area is 93 km² and consists of a mixture of managed coniferous forest, mires and lakes. Human activities in the catchment consist of forestry, with a number of small gravel roads crossing through the area, and some small settlements, which include smaller parcels of agricultural land (Figure 1).

[9] Stor-Strömsjön has a lake area of 3.5 km², which is divided into two main basins: a smaller and shallower eastern basin (1.1 km²; maximum depth 4.2 m) and a larger and deeper western basin (2.4 km²). The western basin can be sub-divided further into two sub-basins, one larger section in the northern end (maximum depth 8.2 m), and a smaller section in the southern end (maximum depth 11.8 m), hereafter referred to as the northwestern and southwestern basins, respectively. While smaller streams and ditches feed into the eastern and southwestern basins, the main inlet, which drains $\sim 64\%$ of the lake's catchment, feeds into the northwestern basin. The only outlet is located on the south-eastern end of the eastern basin and it has a small dam that has raised the water level of the lake by about 0.5 m.

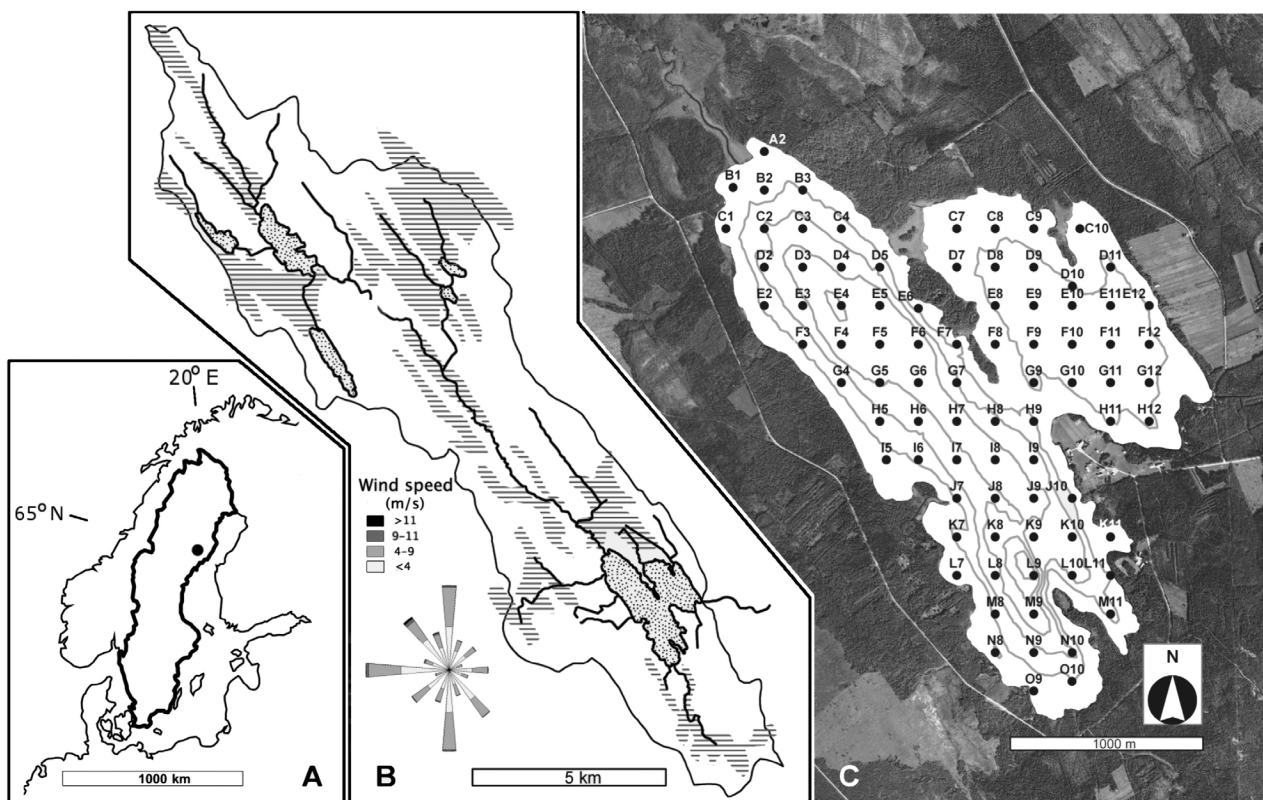


Figure 1. Maps of Stor-Strömsjön and its surroundings. (a) The location of Stor-Strömsjön in Scandinavia. (b) A schematic map over the Stor-Strömsjön catchment with lakes, mires and larger streams indicated. The wind rose indicates the predominant wind directions. (c) An aerial photograph of the lakes immediate surrounding combined with a bathymetric map over the lake where the 83 sample locations have been marked. Contour intervals in the bathymetric map are 2 m.

2.2. Sampling

[10] Surface sediment samples from Stor-Strömsjön were collected in January 2009. A Geodolite total station was used to mark a 200 by 200 m grid on the lake ice, resulting in 85 potential sample locations. Two locations were removed because the sediment was too compact for sampling (F2 and G13), thus yielding a total of 83 sample locations. Water depth was recorded for each location, and the slope at each location was thereafter modeled using ArcGIS (www.esri.com). At each location the top 2 cm of the sediment was sampled using a HTH-gravity corer [Renberg and Hansson, 2008]. A 0–2 cm sample provides enough material (2 g) for the analyses used, but at the same time it restricts the period during which the sediment has accumulated as much as possible. This is important for two reasons: first, a thin sample reduces the effect of differences in sediment accumulation rate across the lake basin, and second, a thin sample represents sediments in close connection with the water column that are more relevant for biogeochemical cycling of elements. Even so it is necessary to keep in mind that the top 2 cm of the sediment represent different time spans in different locations, and thus, it might be more or less affected by temporal changes in the Hg-loading. The samples were transferred in the field into new polypropylene boxes with polyethylene lids. In the lab all samples were weighed, freeze-dried, re-weighed to calculate dry bulk

density (B.D.), and then homogenized and powdered prior to further analysis. The samples were stored in a dark freezer (-20°C) both before and after freeze drying to minimize any risk of organic matter degradation that could affect the FTIRS analysis.

2.3. Analysis

2.3.1. WD-XRF

[11] A Bruker Tiger S8, WD-XRF analyzer was used to determine the elemental concentrations of selected major (Na, Mg, Al, Si, K, Ca, P, S, Mn, Fe) and trace elements (Cl, Sc, Ti, V, Cr, As, Br, Y, Zr, Ni, Cu, Zn, Rb, Sr, Ba, Pb) in all 83 samples. About 2 g of powdered sediment material was analyzed and elemental concentrations were calculated using a calibration method specifically designed for lake sediments (modified from De Vleeschouwer *et al.* [2011]). Lower limits of detection (LLD) range from a few ppm for most trace elements to a few tens of ppm for major elements. Accuracy –assessed using 10 different CRM’s – was within $\pm 10\%$ for K, Ca, Al, Si, Ti, Mn, Rb, Sc, Cl, Y, Cu, Zn, Ni and V, 10–17% for Na, Fe, Ba, Sr, Zr, S, As and Pb, and above 20% for Mg, Br, P and Cr. However, for most elements the reproducibility for replicate samples ($n = 3$) is within $\pm 5\%$, with the exception of Sc, Br, As and Cr, which have reproducibilities of $\pm 8, 10, 36$ and 12% , respectively.

Values for LLD, accuracy and reproducibility are provided in the auxiliary material.¹

2.3.2. Carbon and Nitrogen

[12] C and N concentrations were determined simultaneously using a Perkin Elmer 2400 Series II CHNS/O-analyzer (operated in CHN-mode). The accuracy of reference samples ($n = 28$) was within $\pm 10\%$ and sample replicates ($n = 24$) were always within $\pm 10\%$ of each other. The C and N concentrations are reported as percent of sediment dry mass, and due to the non-calcareous bedrock in the area, total C can be considered to be equal to organic C. This assumption was also supported by the FTIRS spectra, where no peaks appear in spectral regions known to be associated with carbonates [Rosén *et al.*, 2010].

2.3.3. FTIRS

[13] As a complement to the more traditional WD-XRF and elemental analysis, we also subjected the samples to FTIRS analysis. FTIRS uses the mid-infrared region and is sensitive to both inorganic constituents (primarily Fe, Mn, Si, carbonates and clay minerals), as well as, organic matter [Belzile *et al.*, 1997; Farmer, 1974]. In this study FTIRS is primarily used to infer biogenic silica (BSi) and to assess whether there are any differences in organic matter quality between different parts of the lake, however, it is also used as supportive data for the data obtained with WD-XRF analysis.

[14] FTIRS analysis followed the procedure of Vogel *et al.* [2008]. In brief: The sediment was mixed with potassium bromide (KBr, Spectroscopic grade, Fisher Scientific), and FTIR spectra were obtained under vacuum using a Bruker IFS 66v/S FTIR spectrometer (Bruker Optik GmbH, Germany) equipped with a diffuse reflectance accessory (Harrick Inc., USA). FTIR spectra were obtained between 400 and 3750 cm^{-1} . All spectra were baseline corrected using two points, i.e., 2200–2210 and 3750 cm^{-1} in order to reduce the effect of possible instrumental drift.

2.3.4. FTIRS Inferred Biogenic Silica

[15] Biogenic silica (BSi) has a different FTIRS signature as compared to geogenic Si [Gendron-Badou *et al.*, 2003], and Rosén *et al.* [2011] have developed a method for inferring BSi from the FTIR spectra. In brief: The FTIR spectra of 816 sediment samples with known BSi concentrations (ranging from 0 to 55% as determined according to the method of Müller and Schneider [1993]). Using the software SIMCA-P 10.0 (Umetrics AB, SE-907 19 Umeå, Sweden), a 4-component PLS model including spectral regions with known molecular vibrations of BSi (435–480, 790–830 and 1050–1280 cm^{-1}) was developed [Gendron-Badou *et al.*, 2003]. The model between the conventionally measured BSi and FTIRS-inferred BSi shows a cross-validated predictive power (R_{cv}) of 0.93.

2.3.5. Mercury

[16] Total-Hg concentrations were determined using a Leco AMA 254-analyzer (thermal decomposition-atomic absorption spectrometer). Calibration was based on analyses of different weights (20–200 mg) of MESS-3 (National Resources Canada, certified value $91 \pm 9 \text{ ng g}^{-1}$). CRMs were included along with the samples, and were within their respective certified ranges and all sample replicates ($n = 23$) were within $\pm 10\%$.

2.3.6. Methylmercury

[17] Based on the WD-XRF results, a sub-set of 35 samples was selected for methyl-Hg analysis. In the selection procedure the aim was to retain as much as possible of the variability in the entire 83-sample data set, and also to have a reasonable spatial coverage within the lake basin. Methyl-Hg was analyzed according to the isotope dilution method described in Lambertsson *et al.* [2001]. The method precision was 5% RSD, based on replicate sample analyses ($n = 3$), and the method detection limit was 0.03 ng MeHg g^{-1} , calculated as 3-times the standard deviation (3σ) of the blank.

2.4. Statistical Analysis

[18] All statistical analyses of the Stor-Strömsjön data were done using the SPSS software package PASW, version 18.0 (www.spss.com). Bi-variate correlation coefficients (r) were calculated as 2-tailed Pearson correlations and only correlations significant at the 0.05-level or above are reported. To distinguish bi-variate correlations from PC-loadings, which are reported as percent of variance explained, the correlation coefficients are given as r^2 -values. Due to a non-normally distributed sample population within clusters, the statistical significance of any differences in Hg between clusters was evaluated using an independent-sample Kruskal-Wallis test with the significance level set to 0.05. Prior to PCA and cluster analysis all data (also the PC_{FTIR} scores) were converted to Z-scores (with average = 0 and variance = 1).

2.4.1. Cluster Analysis

[19] The observations (sample locations) are grouped into distinct clusters based on their geochemical composition. This makes it easier to identify the general patterns in sediment distribution in the lake, and to look beyond individual sample locations and individual variables. A geochemical data set, consisting of the WD-XRF data and the C, N, inferred BSi and bulk density, was subjected to a hierarchical agglomerative cluster analysis using Wards linkages [Ward, 1963] based on squared Euclidean distances; a solution of 5 clusters was selected to represent the data.

2.4.2. Principal Component Analysis

[20] FTIRS produce a large quantity of data – 1738 spectral absorbance points – for each sample and because our intention is to use the FTIRS data together with the WD-XRF data in subsequent principal component analysis (PCA), there is a need to reduce the number of variables (otherwise the FTIRS data will totally dominate the PCA), but still retain as much as possible of the information regarding the sediment composition. This was achieved by first subjecting the FTIRS data alone to a PCA (PCA_{FTIR}). In this initial PCA we extracted variables with eigenvalues > 10 , and used a Varimax rotated solution, which resulted in the extraction of six principal components (PC_{FTIR}) explaining 98% of the total variance.

[21] The scores of the six PC_{FTIR} were then used as variables, together with the WD-XRF elemental data, water depth, basin slope, inferred BSi, C, N, total-Hg and methyl-Hg data, in two separate PCAs. The first was done using all 83 sample locations, but excluding methyl-Hg as a variable (PCA_{All}), while the second included only the reduced set of 35 locations where both tot-Hg and methyl-Hg were measured (PCA_{Red}). In both PCAs all components with eigenvalues > 1 were extracted using a Varimax rotated solution [Kaiser, 1958]. This type of rotation reduces the number of

¹Auxiliary materials are available in the HTML. doi:10.1029/2012JG001992.

Table 1. Minimum, Maximum and Whole-Lake Average Concentrations for All Variables Analyzed With WD-XRF, FTIRS-Inferred BSi, Bulk Density (B.D.), C, N, Water Depth (W.D.) and Slope

Variable	Unit	Whole-Lake Values			Cluster Average ^a				
		Min	Max	Average	1 (n = 9)	2 (n = 10)	3 (n = 22)	4 (n = 22)	5 (n = 20)
Na	ppm	1716	10714	3777	<i>6741</i>	<i>5383</i>	2894	3921	2452
Mg	ppm	2702	9303	6058	<i>6827</i>	<i>8626</i>	5239	<i>6722</i>	4598
K	ppm	3234	8837	5887	<i>7556</i>	<i>8186</i>	5017	6380	4402
Ca	ppm	4569	13362	7550	<i>10759</i>	<i>8727</i>	6977	7629	6059
Al	%	1	2.7	1.8	2.2	2.5	1.6	2	1.4
Si	%	15.6	30.8	23.2	<i>26.6</i>	24.8	18.2	23.6	26
Ti	ppm	955	3440	2310	<i>2993</i>	<i>3197</i>	1925	2519	1754
Fe	%	1	11.4	5.3	2.4	3.1	8.7	4.6	4.8
Mn	ppm	445	59542	9586	2602	2359	<i>20760</i>	6774	7142
Ba	ppm	295	1995	1210	<i>1663</i>	<i>1710</i>	1198	1122	864
Rb	ppm	31	120	70	<i>91</i>	<i>107</i>	53	77	55
Sr	ppm	49	207	94	<i>157</i>	<i>124</i>	77	96	70
Sc	ppm	4	11	7	9	10	6	8	6
Y	ppm	13	28	21	25	25	18	22	20
Zr	ppm	76	390	143	<i>257</i>	<i>183</i>	114	143	106
S	%	0.03	0.14	0.08	0.06	0.06	0.06	0.08	<i>0.1</i>
P	ppm	75	1360	440	288	410	439	535	422
Cl	ppm	57	158	102	90	93	94	104	<i>119</i>
Br	ppm	3	30	15	8	11	15	15	<i>21</i>
As	ppm	0	185	64	21	16	<i>118</i>	48	64
Cu	ppm	4	18	12	8	<i>16</i>	9	<i>14</i>	<i>14</i>
Zn	ppm	43	236	123	77	132	136	122	127
Pb	ppm	0	36	23	20	26	17	22	29
Ni	ppm	12	39	23	20	31	22	25	21
V	ppm	36	79	58	57	74	54	64	48
Cr	ppm	63	921	228	203	129	362	199	172
BSi	%	0.04	24.5	10.4	5	7.2	6.9	9.9	<i>18.6</i>
B.D.	g cm ⁻³	0.038	0.591	0.095	<i>0.209</i>	0.097	0.099	0.067	0.07
C	%	1.6	11.9	8	5.6	6.8	7.5	8.4	<i>9.7</i>
N	%	0.1	1	0.6	0.4	0.5	0.5	0.6	<i>0.8</i>
W.D.	m	0.6	11.4	3.9	2.3	7.2	3.5	4.7	2.1
Slope	°	0	17.4	1.0	0.8	0.3	2.2	0.5	0.8

^aListed are also the averages values for each of the variable for each of the 5 clusters defined in Figure 2. For the cluster averages: italics denote values above whole-lake average (>10% above); boldface denotes values close to whole-lake average ($\pm 10\%$); and nonbold, nonitalic entries are values below whole-lake average (>10% below).

components used to explain each variable and results in cleaner, and more easily interpreted, factor loadings. Factor loading coefficients (loadings) were calculated as regression coefficients, which is analogous to r in Pearson correlations. For convenience the loadings are reported as percent of variance explained, i.e., as squared loadings. For all PCs, variables with loadings less than 15% were considered to be insignificant with respect to that PC, and hence, they are not further discussed in relation to that particular PC.

3. Results and Discussion

3.1. Sediment Geochemistry

[22] If some shallow locations with very low organic content are excluded the sediments of Stor-Strömsjön are relatively rich in organic matter (8.2% C, excluding cluster-1 locations). However, when subjected to cluster analysis, five different types of sediments, with different geochemical characteristics, can be identified (Table 1 and Figure 2). Together with the statistical association between different elements identified by the PCA's, this allows for making an interpretation of the major factors affecting sediment distribution in Stor-Strömsjön.

3.1.1. The PCAs

[23] For the whole 83-sample data set (PCA_{All}) seven principal components (PC_{All} 1–7) were extracted, which

together explain 89% of the total variance in sediment composition (Figure 3). In the reduced 35-sample PCA (PCA_{Red}) six PCs were extracted (PC_{Red} 1–6), also explaining 89% of the total variance (Figure 4). The general patterns in PCA_{All} and PCA_{Red} are very similar, especially for tot-Hg, which indicates that the 35-sample sub-set selected for methyl-Hg analysis is representative for the whole-lake data set (83 locations). Here follows a short description of the seven PC_{All}. Because the first three PCs are basically the same for both PCA_{All} and PCA_{Red}, no difference is made between PC_{All} 1–3 and PC_{Red} 1–3. For the remaining four (or three) PCs, they will be introduced using the order in which they appear in PCA_{All}, with a reference to the corresponding PC_{Red}.

3.1.1.1. PC-1: Mineral Composition

[24] The first PC (explaining 33 and 34% of total variance for PC_{All} and PC_{Red}, respectively) separates the sediment matrix into two minerogenic fractions. Positive loadings represent high concentrations of elements generally associated with silicate minerals (Mg, Al, Rb, K, Ti, Sr, Zr, Si), and thus, it indicates samples rich in silicates. Negative loadings represent higher concentrations of Fe, As, Mn, Zn together with C and Br. This is consistent with negative PC-1 scores being indicative of samples rich in Fe-/Mn-precipitates, which are known to often contain trace metals and organic matter due to co-precipitation during their formation

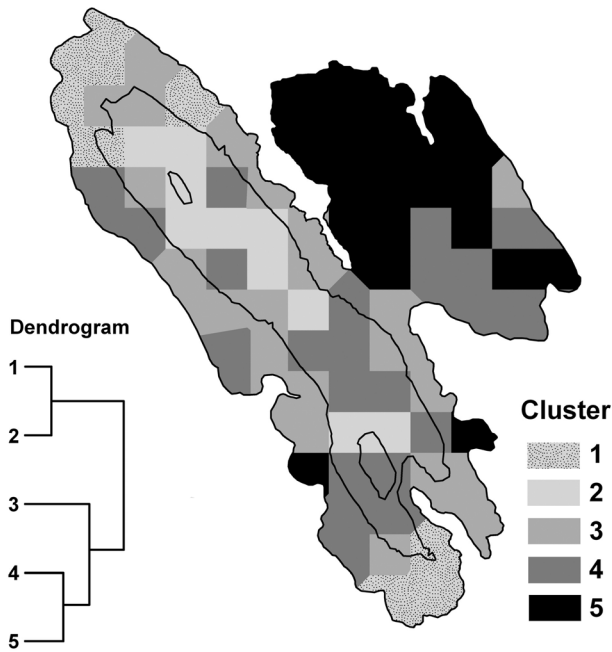


Figure 2. A dendrogram showing the relationship between the five clusters identified in the cluster analysis (left), and the spatial distribution of the different clusters across the lake basin (right). Contour intervals are 4 m.

[Deer et al., 1992; Du Laing et al., 2009; Guo et al., 1997]. That PC_{FTIR-1} loads together with Fe, As, Mn and Zn and orthogonally to Si, is consistent with the FTIR spectra, where locations with negative PC_{FTIR-1} have high spectral intensities in regions important for Si (e.g., a large peak centered at 1000 cm^{-1} [Ellerbrock et al., 1999]).

3.1.1.2. PC-2: Organic Matter

[25] For the second PC (explaining 21% of total variance for both PC_{All} and PC_{Red}), elements that are either a part of,

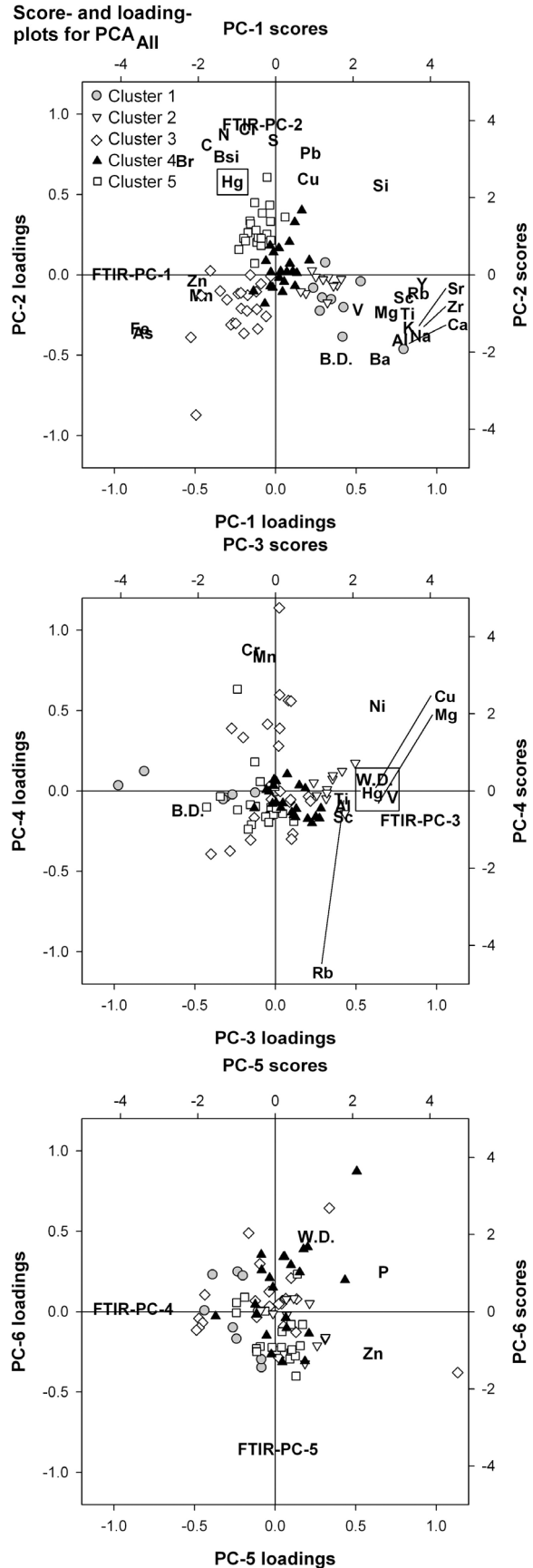
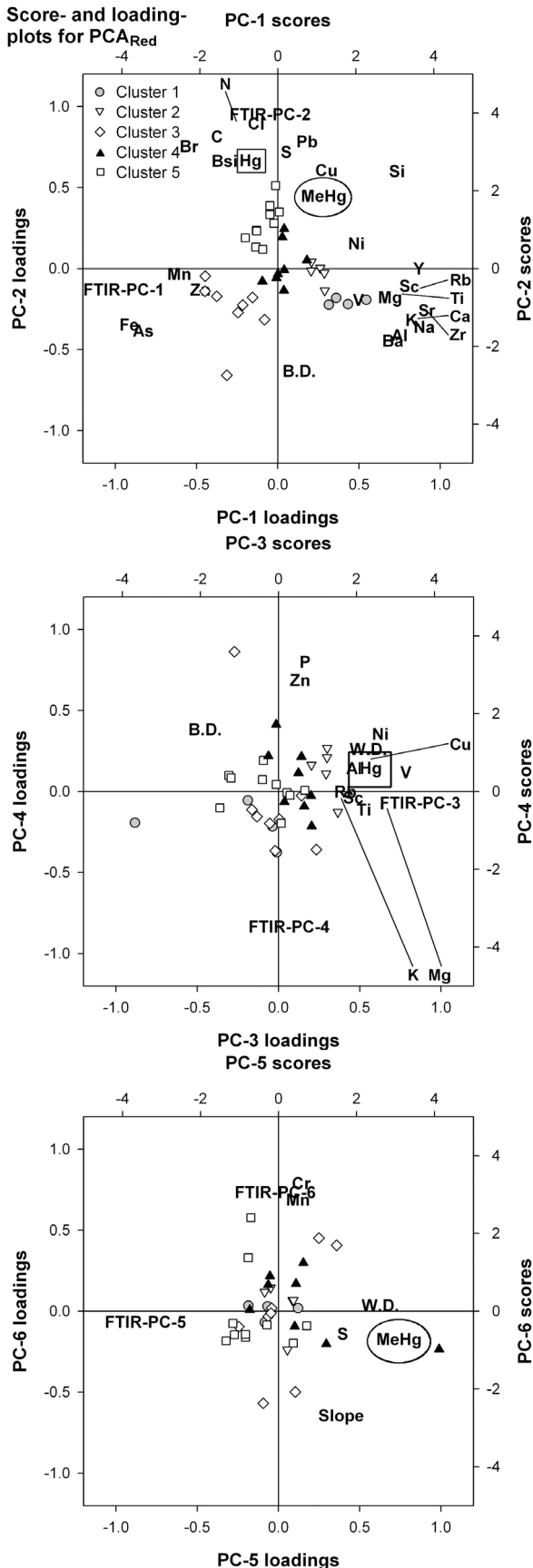


Figure 3. Combined score- and loading-plots for PCs 1–6 depicting how different variables and samples relate to each other in the ordination space as defined by PCA_{All} (PCA using all 83 samples, but excluding MeHg; PC-7 not shown; cf. Figure 4). In brief, PC-1 is related to mineral composition (Fe/Mn-precipitates versus silicate minerals), PC-2 is related to the amount of organic matter, PC-3 relates to the mineral matter grain size and PC_{All-6} is related to water depth (the actual process behind PC-4 and 5 is less clear). Total-Hg plots mainly on the positive side of PC 2 and 3 (indicated by squared boxes), indicating that high total-Hg concentrations can be linked to higher amounts of organic matter and/or fine-grained mineral matter. The five different clusters represent samples characterized by: (1) coarse-grained minerogenic sediments with very low organic content, (2) fine-grained minerogenic sediments with low organic matter content, (3) Fe/Mn-precipitates, (4) a composition close to the whole-lake average and (5) higher organic matter content. To make the figures more legible all variables with PC-loadings of less than 0.39 for both plotted PCs have been removed and overlapping elements have been moved to the edge of the plot with lines marking their actual location.



or are strongly associated with, organic matter have positive loadings (C, N, Cl, Br, S, BSi, Pb, Cu, Hg) together with PC_{FTIR-2}. FTIR spectra from locations with positive PC_{FTIR-2} scores show high spectral intensities in regions important for organic matter and BSi (e.g., 1100, 1300–1750 and 2800–3000 cm⁻¹ [Gendron-Badou et al., 2003; Mecozzi and Pietrantonio, 2006]). On the negative side of PC-2 we find bulk density together with some of the major constituents of minerogenic material (Ca, Al). However, PC-2 is not merely a measure of the organic matter concentrations (e.g., some of the C is associated with PC-1); it also tends to separate differences in organic matter quality. This is indicated by the positive loading for BSi – which mostly originates from algal material with high carbon quality, as compared to terrestrial organic matter – and a negative bivariate correlation between the PC-2 scores and C:N-ratio ($r^2 = 0.44$). The C:N-ratios can be seen as a proxy for organic matter quality with low C:N values (4–10, atomic ratio) indicating fresh organic matter mostly produced within the lake and high values (>20) representing more degraded organic matter of terrestrial origin [Meyers and Teranes, 2001]. That Si loads on the positive side of this component can be explained by BSi being a significant part of the total Si-pool in Stor-Strömsjön.

3.1.1.3. PC-3: Mineral Matter Grain Size

[26] In the third PC (explaining 12 and 13% of total variance for PC_{All} and PC_{Red}, respectively) there is a split between water depth, some trace elements (Ti, K, Rb, Hg, Cu, Ni, V) and Mg on the positive side, and bulk density on the negative. On the positive side of the loading plot we also find PC_{FTIR-3}. We suggest that PC-3 separates between coarse- and fine grained minerogenic sediments, because elements known to be enriched in the fine-grained clay

Figure 4. Combined score- and loading-plots for PCs 1–6 depicting how different variables and samples relate to each other in the ordination space as defined by PCA_{Red} (PCA using only 35 samples, but all variables including MeHg; cf. Figure 3). In brief, PC-1 is related to mineral composition (Fe/Mn-precipitates versus silicate minerals), PC-2 is related to the amount of organic matter, PC-3 relates to the mineral matter grain size and PC_{Red}-5 is related to water depth and possibly anoxia (the actual process behind PC-4 and 6 is less clear). Total-Hg plots mainly on the positive side of PC 2 and 3 (indicated by squared boxes), indicating that high total-Hg concentrations can be linked to higher amounts of organic matter and/or fine-grained mineral matter (cf. Figure 3). Methyl-Hg is mainly associated with PC_{Red}-5, but also to some extent to PC-2 (indicated by ellipses). This indicates that the main factor controlling methyl-Hg is water depth and that organic matter content is of only limited importance. The five different clusters represent samples characterized by: (1) coarse-grained minerogenic sediments with very low organic content, (2) fine-grained minerogenic sediments with low organic matter content, (3) Fe/Mn-precipitates, (4) a composition close to the whole-lake average and (5) higher organic matter content. To make the figures more legible all variables with PC-loadings of less than 0.39 for both plotted PCs have been removed and overlapping elements have been moved to the edge of the plot with lines marking their actual location.

fraction, for example, Ti, K and Rb, [Koinig *et al.*, 2003; Taboada *et al.*, 2006], have positive loadings, while bulk density, which is favored by a coarser grain size, has a negative loading. That water depth plots on the positive side would be consistent with the general model for sediment focusing, where fine-grained material tends to accumulate in deeper waters [Håkanson and Jansson, 1983]; and a finer grain size would give a larger negatively charged surface area, as compared to coarser-grained material, and thus a greater ability to adsorb trace metals such as Hg, Cu, Ni and V [Stone and Droppo, 1996].

3.1.1.4. PCs 4 to 7

[27] PC_{All-4} (PC_{Red-6}; both accounting for 7% of total variance) is mainly driven by changes in Cr and Mn, which both have a strong positive loading (for PC_{Red-6} also PC_{FTIR-6} is a strong driver). For PC_{All-5} (PC_{Red-4}; 6 and 7% of total variance, respectively), P and Zn are the main drivers. PC_{All-6} (PC_{Red-5}; 5 and 7% of total variance, respectively) is driven by water depth, which has a positive loading, and PC_{FTIR-5}, which has a negative loading. In PC_{Red-5} methyl-Hg also plots on the positive side, together with water depth and S. For PC_{All-7} (4% of total variance) the driving variables are PC_{FTIR-6}, with a positive loading, and basin slope, with a negative loading. PC_{Red-6} represents a combination of PC_{All-4} and PC_{All-7}, and has positive loadings for Cr, Mn and PC_{FTIR-6}, and a negative loading for basin slope.

3.1.2. Spatial Patterns in the Sediment Geochemistry

[28] The surface sediments from shallow locations close to the major inlet in the northwestern basin and minor inlets in the southwestern basin (cluster 1) have higher than whole-lake average concentrations of major elements (e.g., Na, Mg, K, Ca, Al, Si), higher bulk density and low trace metal and organic matter concentrations (Table 1 and Figure 2). Taken together with the positive PC-1 and negative PC-2 and PC-3 scores, this indicates coarser-grained minerogenic sediments mainly consisting of silicate minerals (Figures 3 and 4). This shows, as would be expected, that the inlets – particularly the main inlet – are major sources for silicate minerals to Stor-Strömsjön, and that the lighter fraction is depleted in these shallow areas due to water action [Håkanson and Jansson, 1983].

[29] In the deeper areas of the northwestern basin (cluster 2) the surface sediment has similar concentrations for major elements as compared to cluster 1. Hence, cluster-2 locations plot on the positive side of PC-1 and negative side of PC-2, indicating that they consist of the same type of silicate minerals as cluster 1 (Table 1 and Figures 2–4). However, the surface sediments within cluster 2 have positive PC-3 scores and are enriched in several trace metals (i.e., Hg, Cu, Pb, Ni, V), which suggests a more fine-grained material. This would comply with a transport of fine-grained material from shallower to deeper areas of the northwestern basin [Håkanson and Jansson, 1983]. That fine-grained minerogenic rich sediment (cluster 2) is mainly confined to the deep areas of the northwestern basin – as opposed to the more organic rich sediments found in the southwestern (cluster 4) and eastern (cluster 5) basins – supports the idea that the main inlet, which drains 64% of the lake's catchment, is the main supplier of silicate mineral material to the lake.

[30] Along the shorelines of the two western basins (cluster 3) the surface sediments are generally rich in Fe and Mn, and have negative PC-1 and PC-2 scores and plot in the

middle of PC-3 (Table 1 and Figures 2–4). This indicates a material high in Fe/Mn-minerals, which also is consistent with the presence of visually identifiable grains of Fe/Mn-precipitates in these samples. That the majority of the cluster-3 locations are found at water depths of 2.4–4 m suggests that the redox conditions in this depth zone – for example, during summer/winter stratification – favor the formation of Fe and Mn precipitates [Stumm and Morgan, 1996]. However, it is also possible that the distribution is linked to inflowing deep groundwater rich in reduced Fe- and Mn-species in these areas [Stumm and Morgan, 1996].

[31] Surface sediments from locations found in the deepest part of the lake, i.e., in the southwestern basin and in the southern end of the eastern basin (cluster 4), have a composition close to the whole-lake average for most elements, and consequently plots in the middle of PC-1, PC-2 and PC-3 (Table 1 and Figures 2–4). A lower relative amount of mineral material in the deep areas of the southwestern, as opposed to the northwestern, basin is consistent with the assumption that silicate mineral material mainly is supplied through the main inlet. For the eastern basin there is a higher input of mineral material to the southern part, as opposed to the northern part, of the basin as a result of water currents transporting mineral material from the western basin toward the outlet.

[32] Locations with surface sediments with higher than average concentrations of organic matter (cluster 5) are generally found in the northern half of the eastern basin, and plot to the positive side of PC-2 and in the middle of PC-1 and PC-3 (Table 1 and Figures 2–4). In-lake production, either pelagic or benthic, is likely an important source of this organic matter given the high concentration of BSi, probably from diatoms. However, the C:N ratio is higher (11–14) than for pure algal material (4–10), and even if differences in nitrogen cycling can affect the C:N-ratio, this indicates that there is also a contribution of terrestrial organic material, presumably through small inlets draining mire areas located north of and along the shores of the eastern basin [Meyers and Ishiwatari, 1993].

[33] Taken separately, each of the three sub-basins complies relatively well to the generalized model of sediment focusing [Blais and Kalff, 1995; Håkanson and Jansson, 1983]. However, on a whole-lake basis there is no correlation between, for example, water depth and organic matter. It is also clear that several locations deviate from the within-basin patterns. This suggests that there is an influence of the catchment properties in the immediate vicinity of these locations [cf. Korsman *et al.*, 1999]. For example, a number of small inlets along the western shore of the northwestern basin, a couple of small mires located near the shore of the southwestern basin and agricultural fields located just east of the eastern basin.

3.2. Total- and Methyl-Hg

[34] For the 83 locations total-Hg concentrations range from 12 to 140 ng g⁻¹, with a whole-lake average of 96 ng g⁻¹ (Table 2 and Figure 5). Total-Hg inventories (i.e., the amount of total-Hg in the top 2 cm per unit area) in the surface sediment also show considerable variation, between 18 and 81 μg m⁻², with a whole-lake average of 39 μg m⁻². In the sub-set of 35 locations, methyl-Hg concentrations vary between 0.07 and 2.45 ng g⁻¹ (whole-lake average,

Table 2. Minimum, Maximum and Whole-Lake Average for Total-Hg Concentration, Total-Hg Inventory, Methyl-Hg Concentration, Methyl-Hg Inventory and MeHg:TotHg Ratio

	Unit	n	All Sample Locations			Cluster Average ^a				
			Min	Max	Average	1	2	3	4	5
Tot-Hg	ng g ⁻¹	83	11.7	137	95.9	46 ^b	<i>109</i>	87^b	<i>107</i>	<i>109</i>
Tot-Hg-Acc	μg m ⁻²	83	18	81	39	38	<i>53^b</i>	36	35	38
MeHg	ng g ⁻¹	35	0.07	2.45	0.70	0.72	0.75	0.42	<i>0.92</i>	0.71
MeHg-Acc	μg m ⁻²	35	0.11	1.37	0.30	<i>0.67</i>	0.32	0.19	0.29	0.25
MeHg:Tot-Hg	%	35	0.20	3.3	0.79	<i>1.6</i>	0.7	0.5	0.8	0.7

^aAverages are also calculated for each of the five clusters defined in Figure 2. For the cluster averages: italics denote values above whole-lake average (>10% above); boldface denotes values close to whole-lake average (±10%); and nonbold, nonitalic entries are values below whole-lake average (>10% below).

^bClusters with average values that differ from all other clusters with statistical significance.

0.70 ng g⁻¹; Table 2 and Figure 5), and methyl-Hg inventories range from 0.11 to 1.37 μg m⁻² (whole-lake average, 0.30 μg m⁻²). The methyl-Hg:total-Hg ratio (MeHg:TotHg) varies between 0.2 to 3.3%, with an average ratio of 0.79% for the whole lake.

3.2.1. Total-Hg in Surface Sediments of Stor-Strömsjön

[35] In both PCA_{All} and PCA_{Red} two principal components, together explaining ~70% of the total-Hg variance, are of almost equal importance for explaining total-Hg concentrations in surface sediments from Stor-Strömsjön (Figures 3 and 4). One PC is associated to organic matter

(PC-2; 34 and 43% for PCA_{All} and PCA_{Red}, respectively) and the other to fine-grained mineral matter (PC-3; 36 and 33% for PCA_{All} and PCA_{Red}, respectively). That such a large part of total-Hg is statistically associated with mineral matter is interesting, and partly contradicts the general assumption that total-Hg in the boreal landscape is almost exclusively controlled by organic matter [Meili, 1991; Ullrich et al., 2001]. Even so, the capacity for mineral particles to adsorb Hg is well documented [Gabriel and Williamson, 2004; Schuster, 1991], especially if the mineral grains are coated with organic substances, for example,

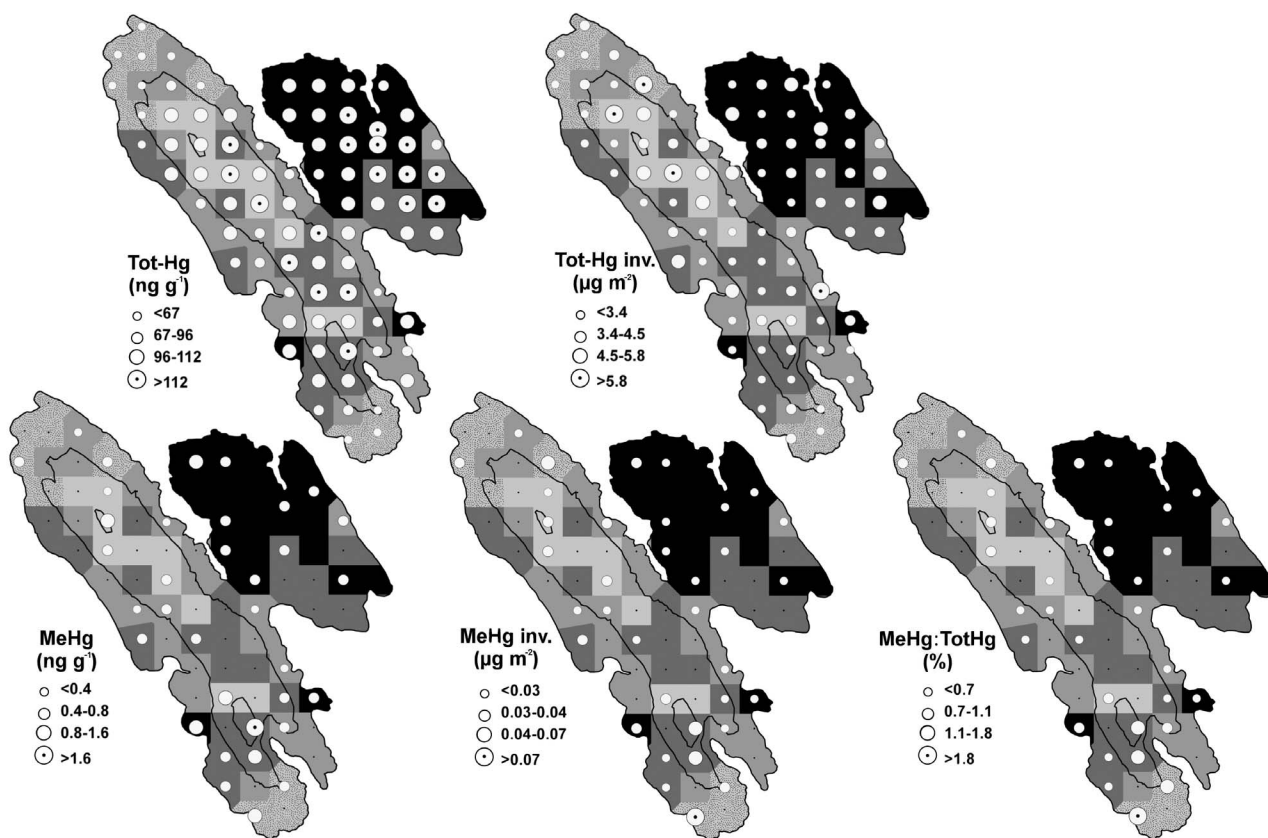


Figure 5. The spatial distribution of total-Hg concentration, total-Hg inventories, methyl-Hg concentration, methyl-Hg inventories and methyl-Hg:total-Hg ratio. Ranges for the symbol classes are defined using natural breaks in the sample distribution (as defined by ArcGIS; www.esri.com). To make it easier to relate the spatial distribution of the Hg data it has been overlain on the cluster map from Figure 2. Contour intervals are 4 m.

fulvic acids [Bäckström *et al.*, 2003]; and a strong connection between fine-grained mineral matter and total-Hg concentrations is reported from studies conducted in areas outside of the boreal region [Roulet *et al.*, 2000; Yin and Balogh, 2002].

[36] If the spatial patterns of total-Hg in surface sediments are studied based on the cluster analysis it is interesting to note that there are no significant differences in total-Hg concentrations between clusters 2, 4–5, even if the sediment composition is different (more minerogenic, intermediate and more organic, respectively). This suggests that, even though the two PCs that are equally important for explaining total-Hg on a whole-lake basis, they have a different relative importance in different parts of the lake. This can be assessed by looking at the bi-variate correlation between total-Hg versus C (a proxy for organic material) and total-Hg versus PC-3 scores (the grain-size related PC), which provide an assessment of the predictive power of C and PC-3, respectively, for total-Hg concentrations. If all sample locations are included in the correlation analysis, the regression line has an r^2 of 0.44 and 0.35 for total-Hg versus C and total-Hg versus PC-3, respectively. However, if the cluster-2 locations – sediments rich in fine-grained mineral material – are removed from the total-Hg versus C correlation then the r^2 increases from 0.44 to 0.58. And similarly, if the cluster-5 locations – sediments rich in organic matter – are removed from the total-Hg versus PC-3 correlation the predictive power of fine-grained mineral material increases from 0.35 to 0.55. These spatial patterns support the notion from the PCA that both organic matter and fine-grained mineral matter are important transport vectors for total-Hg into and within Stor-Strömsjön. The main transport route for mineral bound total-Hg likely is through the main northern inlet, whereas the origin of the organically bound total-Hg can be linked to two separate, but intertwined, processes. First, total-Hg can be transported to the lake along with terrestrial organic material from the catchment, both through the main inlet but maybe more importantly from the smaller inlets draining mire areas in close proximity to the lake (e.g., around the northern side of the eastern basin). Second, Hg atmospherically deposited directly on the lake surface can bind and settle with organic matter in the water column [Hines and Brezonik, 2007; Meili, 1991; Outridge *et al.*, 2007].

[37] For total-Hg concentrations organic matter and fine-grained mineral material are of equal importance, but if the total-Hg inventories (i.e., the amount of tot-Hg in the upper most 2 cm) is considered, the most important transport route for total-Hg is likely together with fine-grained mineral material entering the lake through the main inlet. This idea is supported by cluster 2 having significantly higher total-Hg inventories as compared to other clusters (Table 2). That an increased catchment to lake area ratio increases the total-Hg loading is well known from other studies, for example, Swain *et al.* [1992], but it is interesting that the difference between the eastern and northwestern basins – where the northwestern basin has a considerably larger catchment to lake area ratio – might be linked to differences in the sediments geochemical composition.

[38] Total-Hg in hypolimnetic waters and sediments has previously been linked to other elements, for example, Fe and Mn [Chadwick *et al.*, 2006; Regnell *et al.*, 2001]. However, in the case of Stor-Strömsjön no such links could

be made, possibly due to the large differences in mineralogical composition between sampling locations – for example, very high concentrations of Fe/Mn-precipitates in some locations – which might cloud any such relationship present in deeper, more anoxic waters.

3.2.2. Sediment Distribution of Methyl-Hg

[39] Whereas total-Hg concentrations are largely controlled by a combination of organic and fine-grained mineral matter (PC-2 and PC-3), most of the variance in methyl-Hg concentrations (55%) is explained by PC_{Red}-5 (PC_{All}-6). Other variables plotting on PC_{Red}-5 are water depth (39%), S (16%), and PC_{F_{TIR}}-5 (67%). A smaller part, 20%, of the methyl-Hg concentration is associated with PC-2 (organic matter), which also is important for C (66%), total-Hg (45%), S (52%), BSi (44%) and PC_{F_{TIR}}-2 (91%). However, even if both C and total-Hg are correlated to the same PC as methyl-Hg they are not necessarily directly correlated to methyl-Hg. If the variance in methyl-Hg explained by PC_{Red}-5 is removed (i.e., calculating the residuals; Res-MeHg), there is no bivariate correlation between either Res-MeHg and C or total-Hg (p-values of 0.068 and 0.151, respectively). Both for C and total-Hg there are examples of studies in support of both a poor and good correlation between methyl-Hg and these variables; Lambertsson and Nilsson [2006] and Ethier *et al.* [2010] found good correlations between methyl-Hg and C, while, for example, He *et al.* [2007] found the opposite pattern. For methyl-Hg and total-Hg, Ethier *et al.* [2010] also found a good correlation with total-Hg, but Benoit *et al.* [2003] reported a poor correlation.

[40] That methyl-Hg is mostly associated to PC_{Red}-5, which only accounts for 5% of the total variance in sediment composition, indicates that sediment geochemistry is not critically important for the spatial distribution of methyl-Hg in surface sediments from Stor-Strömsjön. This results in a much larger spatial variability in methyl-Hg as compared to total-Hg (Figure 5). It is also reflected by the fact that there are no significant differences in methyl-Hg concentrations between clusters 1–2 and 4–5 (Table 2), and that the four highest methyl-Hg concentrations are found in locations with contrasting surface sediment types; i.e., deep locations rich in both fine-grained mineral matter and organic matter (2.45 and 1.65 ng g⁻¹; cluster 4), a shallow location with organic rich sediments (1.20 ng g⁻¹; cluster 5) and a shallow location with coarse-grained minerogenic sediments (1.15 ng g⁻¹; cluster 1).

[41] Based on these results together with knowledge on the behavior of methyl-Hg and S, it is possible to at least speculate on the controlling mechanisms behind the patterns in methyl-Hg concentrations observed in surface sediments from Stor-Strömsjön. Most of the variance in methyl-Hg concentrations is linked to water depth – which in a dimictic lake could be seen as a proxy for anoxia, which has been shown to be important for methyl-Hg [Benoit *et al.*, 2003; Grigal, 2003; He *et al.*, 2007] – and a fraction (16%) of the S – i.e., an element that is important for methylating sulfur reducing bacteria (SRB) [Benoit *et al.*, 2003; Ullrich *et al.*, 2001]. This suggests that in situ production of methyl-Hg, possibly by SRBs stimulated by anoxia and S, are important for the distribution of methyl-Hg concentrations in Stor-Strömsjön, at least on a whole-lake basis. The co-variation between S and methyl-Hg could also arise simply because S-groups are of importance for the binding of methyl-Hg to organic matter [Qian *et al.*, 2002]. However, if this were the

case we would expect that organic matter also would load on PC-5 (or that a higher portion of the methyl-Hg variation would be explained by PC-2). In fact most of the S (52%), which presumably represents organically bound S, loads on PC-2 (i.e., organic matter), but this PC still only accounts for a smaller part of the methyl-Hg (20%).

[42] Even if PC_{Red-5} is the most important PC for methyl-Hg concentrations, it still only accounts for 55% of the total variance. A part of the remaining variance (20%) is accounted for by PC-2 and organic matter. This association could be due to at least two different processes. One possibility is that the association between methyl-Hg and PC-2 arises from a transport of methyl-Hg from the catchment to the lake, something that is known to be important in some systems [Branfireun *et al.*, 2005]. However, higher PC-2 scores do not only indicate more organic matter, they also indicate a lower C:N ratio, and thus a higher content of algal material which is a better substrate for bacterial growth as compared to terrestrial organic matter [Gudasz *et al.*, 2012]. That methyl-Hg is actually more associated with the quality of carbon than the quantity is also reflected as a weak bivariate correlation between residual methyl-Hg (after removing the explanatory power of PC_{Red-5}) and BSi ($r^2 = 0.20$). Hence, the other possible explanation – and maybe the more likely one based on this data set – is that, in addition to the methylation pathway stimulated by water depth (anoxia) and S, there is a second methylation pathway, which is controlled by organic matter quality. A recent paper by Hamelin *et al.* [2011] also stresses that not only SRBs, but also other microorganisms such as methanogens in shallow waters might be important for the methylation of Hg.

[43] However, even if both PC_{Red-5} and PC-2 are considered this still leaves about 25% of the total variance in methyl-Hg not accounted for. This would imply that there are additional factors, and additional variables, that are important for methyl-Hg distribution in Stor-Strömsjön. These might include the supply of terrestrially produced methyl-Hg, sulfur/Hg-speciation, pore water concentrations of Hg and S, groundwater inflow, microbial activity, demethylation rates and temperature.

[44] As with total-Hg, some spatial patterns emerge when methyl-Hg is viewed in the light of the two most important PCs. The predictability of PC_{Red-5} is reasonably good throughout the lake, but it tends to underestimate the methyl-Hg concentrations in the organic rich sediments of cluster 5 and the two deepest locations within cluster 4 (i.e., the two locations in the western basin with the highest scores on PC-2). If the predictability of PC-2 is assessed in relation to the Res-MeHg (with the effects of water depth and S removed), the performance is better for the cluster-5 locations, but there is still a tendency to underestimate methyl-Hg in the two deepest locations and in locations within cluster 1. This suggests that the PC_{Red-5}, and any process behind this PC, is valid throughout the lake, and that PC-2, and the possible link between methyl-Hg and organic matter quality, is most valid for the sediments of cluster 5. That a part of the unaccounted variance is constrained to shallow locations with highly minerogenic sediments indicates that variables other than those considered in this study are of importance in that particular type of sediment.

[45] For MeHg:THg ratios and methyl-Hg inventories, as compared to concentrations, the within cluster heterogeneity

is even larger and none of the clusters are significantly different from the others. Even so, the highest MeHg:THg ratios and methyl-Hg inventory were found within cluster 1, which also has the highest within-cluster average. All other clusters are close to or slightly below the whole-lake average for methyl-Hg inventories (Table 2 and Figure 5). That the highest inventory of methyl-Hg, and MeHg:TotHg, is found in a shallow location with coarse-grained minerogenic sediments is interesting, and is consistent with what Ethier *et al.* [2010] found in three North American lakes. A large amount of methyl-Hg present in surface sediments in the shallow oxic zone might be an important factor to consider when assessing the bioavailability of methyl-Hg.

4. Conclusions

[46] In Stor-Strömsjön ~70% of the spatial variance in total-Hg concentrations in surface sediments is controlled by the sediment composition, either by the organic matter content or the amount of fine-grained minerogenic material. This emphasizes that not only organic matter needs to be considered when assessing spatial as well as temporal changes in total-Hg concentration in sediments from boreal lakes. For methyl-Hg our interpretation is that in situ methylation is of greatest importance for the observed patterns; however, further studies are needed to better constrain the underlying processes. The other take home message from this study is that there can be significant spatial variability in both concentrations and inventories, especially for methyl-Hg. This is important to recognize both when sediments are used to calculate whole-lake burdens of Hg, and when using concentrations or inventories from single sediment cores to compare different lakes.

[47] Our study also shows that the combination of WD-XRF and FTIRS – two rapid, data-rich analytical techniques – has a large potential for distinguishing different sediment quality, and that these techniques can help to improve our understanding of how elements are distributed in lake basins and what underlying mechanisms account for these distributions. With further development of, for example, calibration models such as for BSi, the FTIRS technique can prove to become even more valuable for biogeochemical studies. Being fast and relatively inexpensive both WD-XRF and FTIRS can also be used to identify interesting patterns in large sample sets, and thereby provide the means to reduce the number of samples needed to be analyzed with more expensive and time consuming techniques, for example, potential methylation, microbial activity, which are needed to more fully understand the behavior of total- and methyl-Hg.

[48] **Acknowledgments.** This study was supported financially by the Swedish Society for Anthropology and Geography (SSAG) through a stipend awarded to the first author. Financial support was also provided by the Faculty of Science and Technology at Umeå University, the Swedish Research Council, FORMAS and the Kempe Foundations. We also thank the students from the Environmental Change Assessment-course in 2009 (Umeå University) for their help during field sampling and initial preparation of the samples, Johanna Engström (Landscape Ecology-group, Umeå University) for her help with the Geodolite total station and Per Person (Department of Chemistry, Umeå University) for the use of their FTIRS instrument.

References

Bäckström, M., M. Dario, S. Karlsson, and B. Allard (2003), Effects of a luvic acid on the adsorption of mercury and cadmium on goethite, *Sci. Total Environ.*, 304(1–3), 257–268, doi:10.1016/S0048-9697(02)00573-9.

- Belzile, N., H. A. Joly, and H. B. Li (1997), Characterization of humic substances extracted from Canadian lake sediments, *Can. J. Chem.*, 75(1), 14–27, doi:10.1139/v97-003.
- Benoit, J. M., C. C. Gilmour, A. Heyes, R. P. Mason, and C. L. Miller (2003), Geochemical and biological controls over methylmercury production and degradation in aquatic ecosystems, in *Biogeochemistry of Environmentally Important Trace Elements*, edited by Y. Cai and O. C. Braids, pp. 262–297, Am. Chem. Soc., Boston, Mass., doi:10.1021/bk-2003-0835.ch019.
- Benoy, G. A., and J. Kalff (1999), Sediment accumulation and Pb burdens in submerged macrophyte beds, *Limnol. Oceanogr.*, 44(4), 1081–1090, doi:10.4319/lo.1999.44.4.1081.
- Bindler, R., I. Olofsson, I. Renberg, and W. Frech (2001a), Temporal trends in mercury accumulation in lake sediments in Sweden, *Water Air Soil Pollut. Focus*, 1, 343–355, doi:10.1023/A:1017561701141.
- Bindler, R., I. Renberg, M. L. Brännvall, O. Emteryd, and F. El-Daoushy (2001b), A whole-basin study of sediment accumulation using stable lead isotopes and flyash particles in an acidified lake, Sweden, *Limnol. Oceanogr.*, 46(1), 178–188, doi:10.4319/lo.2001.46.1.0178.
- Blais, J. M., and J. Kalff (1995), The influence of lake morphometry on sediment focusing, *Limnol. Oceanogr.*, 40(3), 582–588, doi:10.4319/lo.1995.40.3.0582.
- Branfireun, B. A., N. T. Roulet, C. A. Kelly, and J. W. M. Rudd (1999), In situ sulphate stimulation of mercury methylation in a boreal peatland: Toward a link between acid rain and methylmercury contamination in remote environments, *Global Biogeochem. Cycles*, 13(3), 743–750, doi:10.1029/1999GB900033.
- Branfireun, B. A., D. P. Krabbenhoft, H. Hintelmann, R. J. Hunt, J. P. Hurley, and J. W. M. Rudd (2005), Speciation and transport of newly deposited mercury in a boreal forest wetland: A stable mercury isotope approach, *Water Resour. Res.*, 41, W06016, doi:10.1029/2004WR003219.
- Chadwick, S. P., C. L. Babiarz, J. P. Hurley, and D. E. Armstrong (2006), Influences of iron, manganese, and dissolved organic carbon on the hypolimnetic cycling of amended mercury, *Sci. Total Environ.*, 368(1), 177–188, doi:10.1016/j.scitotenv.2005.09.039.
- Chételat, J., M. Amyot, and E. Garcia (2011), Habitat-specific bioaccumulation of methylmercury in invertebrates of small mid-latitude lakes in North America, *Environ. Pollut.*, 159(1), 10–17, doi:10.1016/j.envpol.2010.09.034.
- Croston, N. J., J. M. Bubb, and J. N. Lester (1996), Spatial distribution and seasonal changes in methylmercury concentrations in shallow lakes, *Hydrobiologia*, 321(1), 35–45, doi:10.1007/BF00018675.
- Deer, W. A., R. A. Howie, and J. Zussman (1992), *An Introduction to the Rock-Forming Minerals*, 2nd ed., Longman Sci., New York.
- De Vleeschouwer, F., V. Renson, P. Claeys, K. Nys, and R. Bindler (2011), Quantitative WD-XRF calibration for small ceramic samples and their source material, *Geochronology*, 26(3), 440–450, doi:10.1002/gea.20353.
- Du Laing, G., J. Rinklebe, B. Vandecasteele, E. Meers, and F. M. G. Tack (2009), Trace metal behaviour in estuarine and riverine floodplain soils and sediments: A review, *Sci. Total Environ.*, 407(13), 3972–3985, doi:10.1016/j.scitotenv.2008.07.025.
- Eckley, C. S., and H. Hintelmann (2006), Determination of mercury methylation potentials in the water column of lakes across Canada, *Sci. Total Environ.*, 368(1), 111–125, doi:10.1016/j.scitotenv.2005.09.042.
- Ellerbrock, R. H., A. Hohn, and H. H. Gerke (1999), Characterization of soil organic matter from a sandy soil in relation to management practice using FT-IR spectroscopy, *Plant Soil*, 213(1/2), 55–61, doi:10.1023/A:1004511714538.
- Ethier, A. L. M., A. M. Scheuhammer, J. M. Blais, A. M. Paterson, G. Mierle, R. Ingram, and D. R. S. Lean (2010), Mercury empirical relationships in sediments from three Ontario lakes, *Sci. Total Environ.*, 408(9), 2087–2095, doi:10.1016/j.scitotenv.2009.12.037.
- Farmer, V. C. (Ed.) (1974), *The Infrared Spectra of Minerals*, Mineral. Soc., London.
- Feyte, S., C. Gobeil, A. Tessier, and D. Cossa (2011), Mercury dynamics in lake sediments, *Geochim. Cosmochim. Acta*, 82(1), 92–112, doi:10.1016/j.gca.2011.02.007.
- Fitzgerald, W. F., D. R. Engstrom, R. P. Mason, and E. A. Nater (1998), The case for atmospheric mercury contamination in remote areas, *Environ. Sci. Technol.*, 32(1), 1–7, doi:10.1021/es970284w.
- Fitzgerald, W. F., D. R. Engstrom, C. H. Lamborg, C. M. Tseng, P. H. Balcom, and C. R. Hammerschmidt (2005), Modern and historic atmospheric mercury fluxes in northern Alaska: Global sources and Arctic depletion, *Environ. Sci. Technol.*, 39(2), 557–568, doi:10.1021/es049128x.
- Gabriel, M. C., and D. G. Williamson (2004), Principal biogeochemical factors affecting the speciation and transport of mercury through the terrestrial environment, *Environ. Geochem. Health*, 26(3–4), 421–434, doi:10.1007/s10653-004-1308-0.
- Gendron-Badou, A., T. Coradin, J. Maquet, F. Fröhlich, and J. Livage (2003), Spectroscopic characterization of biogenic silica, *J. Non-Cryst. Solids*, 316, 331–337, doi:10.1016/S0022-3093(02)01634-4.
- Gilmour, C. C., E. A. Henry, and R. Mitchell (1992), Sulfate stimulation of mercury methylation in fresh-water sediments, *Environ. Sci. Technol.*, 26(11), 2281–2287, doi:10.1021/es00035a029.
- Grigal, D. F. (2003), Mercury sequestration in forests and peatlands: A review, *J. Environ. Qual.*, 32(2), 393–405.
- Gudasz, C., D. Bastviken, K. Premke, K. Steger, and L. J. Tranvik (2012), Constrained microbial processing of allochthonous organic carbon in boreal lake sediments, *Limnol. Oceanogr.*, 57(1), 163–175, doi:10.4319/lo.2012.57.1.0163.
- Guo, T. Z., R. D. DeLaune, and W. H. Patrick (1997), The influence of sediment redox chemistry on chemically active forms of arsenic, cadmium, chromium, and zinc in estuarine sediment, *Environ. Int.*, 23(3), 305–316, doi:10.1016/S0160-4120(97)00033-0.
- Håkanson, L., and M. Jansson (1983), *Principals of Lake Sedimentology*, 316 pp., Springer, Berlin, doi:10.1007/978-3-642-69274-1.
- Hamelin, S., M. Amyot, T. Barkay, Y. P. Wang, and D. Planas Methanogens (2011), Principal methylators of mercury in Lake Periphyton, *Environ. Sci. Technol.*, 45(18), 7693–7700, doi:10.1021/es2010072.
- He, T. R., J. Lu, F. Yang, and X. B. Feng (2007), Horizontal and vertical variability of mercury species in pore water and sediments in small lakes in Ontario, *Sci. Total Environ.*, 386(1–3), 53–64, doi:10.1016/j.scitotenv.2007.07.022.
- Hines, N. A., and P. L. Brezonik (2007), Mercury inputs and outputs at a small lake in northern Minnesota, *Biogeochemistry*, 84(3), 265–284, doi:10.1007/s10533-007-9114-2.
- Kainz, M., and M. Lucotte (2006), Mercury concentrations in lake sediments—Revisiting the predictive power of catchment morphometry and organic matter composition, *Water Air Soil Pollut.*, 170(1–4), 173–189, doi:10.1007/s11270-006-3009-z.
- Kaiser, H. F. (1958), The Varimax criterion for analytic rotation in factor analysis, *Psychometrika*, 23(3), 187–200, doi:10.1007/BF02289233.
- Koinig, K. A., W. Shotyk, A. F. Lotter, C. Ohlendorf, and M. Sturm (2003), 9000 years of geochemical evolution of lithogenic major and trace elements in the sediment of an alpine lake—The role of climate, vegetation, and land-use history, *J. Paleolimnol.*, 30, 307–320, doi:10.1023/A:1026080712312.
- Korsman, T., M. B. Nilsson, K. Landgren, and I. Renberg (1999), Spatial variability in surface sediment composition characterised by near-infrared (NIR) reflectance spectroscopy, *J. Paleolimnol.*, 21(1), 61–71, doi:10.1023/A:1008027001745.
- Lambertsson, L., and M. Nilsson (2006), Organic material: The primary control on mercury methylation and ambient methyl mercury concentrations in estuarine sediments, *Environ. Sci. Technol.*, 40(6), 1822–1829, doi:10.1021/es051785h.
- Lambertsson, L., E. Lundberg, M. Nilsson, and W. Frech (2001), Applications of enriched stable isotope tracers in combination with isotope dilution GC-ICP-MS to study mercury species transformation in sea sediments during in situ ethylation and determination, *J. Anal. Atom. Spectrom.*, 16(11), 1296–1301, doi:10.1039/B106878B.
- Likens, G. E., and M. B. Davis (1975), Post-glacial history of Mirror Lake and its watershed in New Hampshire, U.S.A. An initial report, *Verh. Int. Ver. Theor. Angew. Limnol.*, 19, 982–993.
- Lindqvist, O., K. Johansson, M. Aastrup, A. Andersson, L. Bringmark, G. Hovsenius, L. Håkanson, Å. Iverfeldt, M. Meili, and B. Timm (1991), Mercury in the Swedish environment—Recent research on causes, consequences and corrective methods, *Water Air Soil Pollut.*, 55(1–2), 261 pp.
- Mecozzi, M., and E. Pietrantonio (2006), Carbohydrates proteins and lipids in fulvic and humic acids of sediments and its relationships with mucilaginous aggregates in the Italian seas, *Mar. Chem.*, 101(1–2), 27–39, doi:10.1016/j.marchem.2006.01.001.
- Meili, M. (1991), The coupling of mercury and organic matter in the biogeochemical cycle—Towards a mechanistic model for the boreal forest zone, *Water Air Soil Pollut.*, 56, 333–347, doi:10.1007/BF00342281.
- Meyers, P. A., and R. Ishiwatari (1993), Lacustrine organic geochemistry—An overview of indicators of organic matter sources and diagenesis in lake sediments, *Org. Geochem.*, 20(7), 867–900, doi:10.1016/0146-6380(93)90100-P.
- Meyers, P. A., and J. L. Teranes (2001), Sediment organic matter, in *Tracking Environmental Change Using Lake Sediments*, vol. 2, *Physical and Geochemical Methods*, edited by W. M. Last and J. P. Smol, pp. 239–270, Kluwer Acad., Dordrecht, Netherlands.
- Müller, P. J., and R. Schneider (1993), An automated leaching method for the determination of opal in sediments and particulate matter, *Deep Sea Res.*, 40, 425–444, doi:10.1016/0967-0637(93)90140-X.
- Outridge, P. M., H. Sanei, G. A. Stern, P. B. Hamilton, and F. Goodarzi (2007), Evidence for control of mercury accumulation rates in Canadian

- high arctic lake sediments by variations of aquatic primary productivity, *Environ. Sci. Technol.*, 41(15), 5259–5265, doi:10.1021/es070408x.
- Phillips, V. J. A., V. L. St. Louis, C. A. Cooke, R. D. Vinebrooke, and W. O. Hobbs (2011), Increased mercury loadings to western Canadian alpine lakes over the past 150 years, *Environ. Sci. Technol.*, 45(6), 2042–2047, doi:10.1021/es1031135.
- Qian, J., U. Skjellberg, W. Frech, W. F. Bleam, P. R. Bloom, and P. E. Petit (2002), Bonding of methyl mercury to reduced sulfur groups in soil and stream organic matter as determined by X-ray absorption spectroscopy and binding affinity studies, *Geochim. Cosmochim. Acta*, 66(22), 3873–3885, doi:10.1016/S0016-7037(02)00974-2.
- Rada, R. G., D. E. Powell, and J. G. Wiener (1993), Whole-lake burdens and spatial-distribution of mercury in Wisconsin seepage lakes, *Can. J. Fish. Aquat. Sci.*, 50(4), 865–873, doi:10.1139/f93-099.
- Regnell, O., T. Hammar, A. Helgee, and B. Troedsson (2001), Effects of anoxia and sulfide on concentrations of total and methyl mercury in sediment and water in two Hg-polluted lakes, *Can. J. Fish. Aquat. Sci.*, 58(3), 506–517.
- Renberg, L., and H. Hansson (2008), The HTH sediment corer, *J. Paleolimnol.*, 40(2), 655–659, doi:10.1007/s10933-007-9188-9.
- Rhoton, F. E., and S. J. Bennett (2009), Soil and sediment properties affecting the accumulation of mercury in a flood control reservoir, *Catena*, 79(1), 39–48, doi:10.1016/j.catena.2009.05.004.
- Rippey, B., N. J. Anderson, I. Renberg, and T. Korsman (2008), The accuracy of methods used to estimate the whole-lake accumulation rate of organic carbon, major cations, phosphorus and heavy metals in sediment, *J. Paleolimnol.*, 39(1), 83–99, doi:10.1007/s10933-007-9098-x.
- Rosén, P., H. Vogel, L. Cunningham, N. Reuss, D. Conley, and P. Persson (2010), Fourier transform infrared spectroscopy, a new method for rapid determination of total organic and inorganic carbon and biogenic silica concentration in lake sediments, *J. Paleolimnol.*, 43(2), 247–259, doi:10.1007/s10933-009-9329-4.
- Rosén, P., H. Vogel, L. Cunningham, A. Hahn, S. Hausmann, R. Pienitz, B. Zolitschka, B. Wagner, and P. Persson (2011), Universally applicable model for the quantitative determination of lake sediment composition using Fourier transform infrared spectroscopy, *Environ. Sci. Technol.*, 45(20), 8858–8865, doi:10.1021/es200203z.
- Roulet, M., M. Lucotte, R. Canuel, N. Farella, M. Courcelles, J. R. D. Guimaraes, D. Mergler, and M. Amorim (2000), Increase in mercury contamination recorded in lacustrine sediments following deforestation in the central Amazon, *Chem. Geol.*, 165(3–4), 243–266, doi:10.1016/S0009-2541(99)00172-2.
- Rowan, D. J., J. Kalf, and J. B. Rasmussen (1992), Estimating the mud deposition boundary depth in lakes from wave theory, *Can. J. Fish. Aquat. Sci.*, 49(12), 2490–2497, doi:10.1139/f92-275.
- Rypel, A. L., D. A. Arrington, and R. H. Findlay (2008), Mercury in south-eastern U.S. riverine fish populations linked to water body type, *Environ. Sci. Technol.*, 42(14), 5118–5124, doi:10.1021/es8001772.
- Schuster, E. (1991), The behavior of mercury in the soil with special emphasis on complexation and adsorption processes—A review of the literature, *Water Air Soil Pollut.*, 56, 667–680, doi:10.1007/BF00342308.
- Skjellberg, U., P. R. Bloom, J. Qian, C. M. Lin, and W. F. Bleam (2006), Complexation of mercury(II) in soil organic matter: EXAFS evidence for linear two-coordination with reduced sulfur groups, *Environ. Sci. Technol.*, 40(13), 4174–4180, doi:10.1021/es0600577.
- Stone, M., and I. G. Droppo (1996), Distribution of lead, copper and zinc in size-fractionated river bed sediment in two agricultural catchments of southern Ontario, Canada, *Environ. Pollut.*, 93(3), 353–362, doi:10.1016/S0269-7491(96)00038-3.
- Stumm, W., and J. J. Morgan (1996), *Aquatic Chemistry—Chemical Equilibria and Rates in Natural Waters*, 3rd ed., 1022 pp., John Wiley, Hoboken, N. J.
- Swain, E. B., D. R. Engstrom, M. E. Brigham, T. A. Henning, and P. L. Brezonik (1992), Increasing rates of atmospheric mercury deposition in midcontinental North America, *Science*, 257(5071), 784–787, doi:10.1126/science.257.5071.784.
- Taboada, T., A. M. Cortizas, C. Garcia, and E. Garcia-Rodeja (2006), Particle-size fractionation of titanium and zirconium during weathering and pedogenesis of granitic rocks in NW Spain, *Geoderma*, 131(1–2), 218–236, doi:10.1016/j.geoderma.2005.03.025.
- Ullrich, S. M., T. W. Tanton, and S. A. Abdrashitova (2001), Mercury in the aquatic environment: A review of factors affecting methylation, *Crit. Rev. Environ. Sci. Technol.*, 31(3), 241–293, doi:10.1080/20016491089226.
- Vogel, H., P. Rosén, B. Wagner, M. Melles, and P. Persson (2008), Fourier transform infrared spectroscopy, a new cost-effective tool for quantitative analysis of biogeochemical properties in long sediment records, *J. Paleolimnol.*, 40(2), 689–702, doi:10.1007/s10933-008-9193-7.
- Ward, J. H. (1963), Hierarchical grouping to optimize an objective function, *J. Am. Stat. Assoc.*, 58(301), 236–244, doi:10.1080/01621459.1963.10500845.
- Wiener, J. G., B. C. Knights, M. B. Sandheinrich, J. D. Jeremiason, M. E. Brigham, D. R. Engstrom, L. G. Woodruff, W. F. Cannon, and S. J. Balogh (2006), Mercury in soils, lakes, and fish in Voyageurs National Park (Minnesota): Importance of atmospheric deposition and ecosystem factors, *Environ. Sci. Technol.*, 40(20), 6261–6268, doi:10.1021/es060822h.
- Yang, H. D., N. L. Rose, R. W. Battarbee, and J. F. Boyle (2002), Mercury and lead budgets for Lochnagar, a Scottish mountain lake and its catchment, *Environ. Sci. Technol.*, 36(7), 1383–1388, doi:10.1021/es010120m.
- Yin, X. W., and S. J. Balogh (2002), Mercury concentrations in stream and river water: An analytical framework applied to Minnesota and Wisconsin (USA), *Water Air Soil Pollut.*, 138(1/4), 79–100, doi:10.1023/A:1015525729671.